TRENDS IN SCIENCES 2025; 22(2): 8908 RESEARCH ARTICLE
https://doi.org/10.48048/tis.2025.8908

Enhanced Removal of Acetylsalicylic Acid Using Surfactant-Modified Natural Zeolites

Marvince John P. Araneta[1], Ethan Angelo P. Gaw[1],
Christian Gabriel V. Seagan[2], Mark Nathaniel E. Dolina[2], Aldrin P. Bonto[2],
Earl Conan G. Casalme[3], Arnel A. Salvador[3] and Julius Andrew P. Nuñez[1,*]

[1]Laboratory of Materials, Department of Physical Sciences and Mathematics, College of Arts and Sciences,
University of the Philippines Manila, Metro Manila 1000, Philippines
[2]Department Chemistry, De La Salle University, Metro Manila 1004, Philippines
[3]National Institute of Physics, University of the Philippines Diliman, Metro Manila 1101, Philippines

(*Corresponding author's e-mail: jpnunez@up.edu.ph)

Received: 31 August 2024, Revised: 6 October 2024, Accepted: 13 October 2024, Published: 20 December 2024

Abstract

Widely consumed because of its analgesic properties, acetylsalicylic acid and its metabolites are considered as emerging contaminants identified in several regional water sources. Although sophisticated removal techniques such as microbial-degradation and electrochemical-membrane approaches are explored, the search for simpler adsorbent technologies remains popular. In this study, surfactant-modified natural zeolites were developed, characterized, and investigated for its adsorption performance for acetylsalicylic acid. Surfactant-modification using Hexadecyltrimethylammonium-bromide (HDTMA-Br) and Dioctadecyldimethylammonium-bromide (DODA-Br) at 100 and 200 % of the External Cation Exchange Capacity were employed. Zeolite samples were characterized for their thermal, crystallographic, morphological, and physicochemical properties. EDX data, FTIR spectra, and Zeta Potential data confirmed surfactant modification on the surface of the zeolite. XRD showed that modifications did not alter the crystallinity of the zeolites after modification. Batch adsorption experiments were carried out to examine adsorption isotherms in aqueous solutions at pH $\approx$ 7.5. The linearity observed in Freundlich isotherm across all adsorbents suggests heterogenous surface adsorption sites of the base material. Bilayer-DODA-modified zeolites showed significantly promising sorption capacity for acetylsalicylic acid among all adsorbents due to anion exchange, electrostatic interaction, and hydrophobic interaction. This suggests the role of the bilayer and longer carbon chains in influencing adsorbent's affinity towards acetylsalicylic acid.

Keywords: Hexadecyltrimethylammonium-bromide, Dioctadecyldimethylammonium-bromide, Philippine natural zeolites, Acetylsalicylic acid, Adsorption

Introduction

Commonly known as aspirin, Acetylsalicylic acid is one of the widely used over-the-counter non-steroidal anti-inflammatory drugs (NSAIDs) which are considered as emerging class of pharmaceutical contaminants [1-6]. As a biologically active ingredient, it has been reported to have potential reproductive and endocrine disruptive effects and to be a causative agent for antimicrobial resistance [1,4,6,7]. Trace concentrations of acetylsalicylic acid have been detected from water samples obtained from wastewater treatment plants (WWTPs) in almost 15 countries including Japan and Romania despite combining advanced electro membrane and biological approaches [1,8]. Therefore, practical yet effective alternatives must be investigated to address the emerging pollutant.

Natural zeolites are porous aluminosilicate minerals that have been extensively used for removal of inorganic cationic pollutants [2,3,6,7,9-12]. Its adsorption capacity is attributed to zeolites' excellent cation exchange capacity [7,9-11,13,14]. However, its affinity towards organic non-polar species is relatively poor. Alternatively, its cation exchange mechanism can be exploited to modify the surface properties of natural zeolites to facilitate non-polar interactions. This modification involves the use of large organic cations that participate in the cation exchange with the external framework cations of the zeolites [2,3,7,9,10,15,16]. This is popularly known as the cationic surfactant modification which involves adsorbing cationic amphipathic compounds on the surface of the mineral [2,3,7,9,17-20]. Depending on the surfactant concentration, surfactant-modified natural zeolites (SMNZs) can either possess monolayer or bilayer of surfactant molecules [2,3,7,9,10,16,21]. Consequently, this changes the affinity of the surface such that the monolayer attracts hydrophobic species and bilayer attracts anions species [6,7,9,10,22-24].

One-tailed cationic surfactants such as Hexadecyldimethylammonium bromide (HDTMA-Br) have been shown to enhance zeolites in terms of pharmaceutical removal [3,7,9-11,25,26]. This is primarily influenced by the surfactant architecture which denies its entry to zeolite pores due to its bulky alkyl group [27-29]. Moreover, surfactants with larger and more branched hydrocarbon chains can saturate more sites which provides a promising angle in optimizing SMNZs development [30]. To further examine the effect of surfactants' architecture, utilization of two-tailed cationic surfactant is a potential field for development.

The main objective of this study is to develop monolayer and bilayer surfactant modified natural zeolites using one-tailed surfactant with 16-carbon atoms and two-tailed surfactant with 18-carbon atoms, both of which possess a quaternary ammonium head, HDTMA-Br and Dioctadecyldimethylammonium bromide (DODA-Br), respectively. Furthermore, the SMNZs will be characterized to examine its relevant thermal, morphological, physicochemical, and crystallographic properties. Lastly, adsorption isotherms of SMNZs for acetylsalicylic acid removal were modelled to determine their key adsorption parameters.

Materials and methods

Preparation of Sodium Saturated Natural Zeolites

The natural zeolites were provided by Lithos Manufacturing Inc. from Pangasinan, Philippines. The zeolites were subjected to the following modified procedures adopted from literature [16,18,23,31]. Sieved zeolite powders (125 µm) were immersed and cleaned in deionized water at a ratio of 1 g/mL. They were shaken at 180 rpm for 25 min. They were decanted and the process was repeated 4 times. The resulting zeolites were oven dried at 105 °C for 24 h. Dried samples were saturated with 0.3 M NaOH at a ratio of 1 % w/v at 200 rpm for 24 h. Sodium-saturated zeolites (Na-Zs) samples were vacuum filtered with filter paper #1 (90 mm, Whatman) and washed with deionized water. They were oven dried at 105 °C for 24 h and stored in watertight containers.

Determination of External Cation Exchange Capacity (ECEC)

After sodium saturation, determination of ECEC was adopted from literature [2,7,9,25].The Na-Zs were shaken in 20 mM HDTMA-Br at a ratio of 20 % w/v at 200 rpm for 24 h. Mixtures were transferred in 15 mL conical tubes and were centrifuged at 3,000 rpm for 5 min. The supernatants were analyzed using Inductively Coupled Plasma Optical Emission Spectroscopy (ICP-OES) (Prodigy 7, Teledyne, country of manufacturer) to determine Na, K, Ca, Mg cation concentrations. The ECEC was determined using Eqs. (1) and (2);

$$mEq = \frac{mass\ in\ g \times valence}{MW} \tag{1}$$

$$ECEC = \frac{\sum mEq_{cations}}{mass\ of\ zeolite\ in\ g} \tag{2}$$

where mEq refers to milliequivalents.

Surfactant Functionalization

Surfactant functionalization was based on literature [2,3,7,9,18]. Surfactant concentrations of 100 % (5.7 mM) and 200 % (11.4 mM) ECEC for HDTMA-Br and DODA-Br were prepared. The Na-Zs were shaken in their respective surfactant solutions in a ratio of 4 % w/v at 200 rpm for 48 h to produce the SMNZs. The SMNZs were retrieved using vacuum filtration with filter paper #1 and washed with deionized water until no frothing was observed in the liquid. The SMNZs were air dried for 72 h and were stored in watertight containers.

Physicochemical, Thermal, Morphological Characterization of Na-Zs, SMNZs, and D-SMNZs

Zeolite samples were examined using a SU1510 Scanning Electron Microscope (SEM) (Hitachi, Japan); Ultradry 4495B–1UPS–SN Energy Dispersive X-ray (EDX) (Thermo Fisher Scientific, US) to describe the morphological characteristics and elemental surface distribution of the zeolite surface. Prior SEM analysis, samples were coated with platinum for 30 s using a Hitachi MC 1,000 Ion Sputter machine. Micrographs were taken at 15 kV accelerating voltage at 2500x magnification. Data from the elemental analysis was reported as percent element weight taken from the mean of 6 different regions of the sample. Thermal stability of the zeolite was monitored using a 4,000 differential scanning calorimeter (DSC) (PerkinElmer, US) with $N_{2(g)}$ as purge gas at 20 mL/min. DSC measurements of approximately 5 mg of ground zeolite samples loaded in hermetically sealed aluminum pans were taken at 25 to 400 at 10 °C per min heating rate. Zeta potential (ζ) measurements were performed using a Dynamic Light Scattering (DLS) via nanoPartica SZ-100V2 nanoparticle analyzer (Horiba Scientific®, Japan) to confirm surface modifications based on changes in the electric potential at the zeolite-fluid interface. Refractive indices were set at $n_{sample} = 1.465$ and $n_{media} = 1.333$ for ζ measurements. Measurements were taken at triplicates. Functional groups were identified using a IRSpiritTM Fourier Transform Infrared Spectroscopy (FTIR) (Shimadzu®, Japan) coupled with Attenuated Total Reflectance (ATR) accessory of QTAR-S with a diamond reflection crystal. The transmittance spectra were obtained in the 4,000 - 400 cm^{-1} range with 4 cm^{-1} resolution in 64 scans and visualized using IRsolution Ver 2.30 software. Ultimately, the crystallinity of the zeolites was investigated using a Empyrean 3 X-ray diffractometer (XRD) (Malvern PANanalytical, Neatherlands) using 1.5406 Å Cu-Kα radiation. Powder diffractograms were collected from the 2θ range of 3 to 60 ° with a step size of 0.01 ° and the phases were identified using the HighScore Plus version 5.0 software based on the ICDD PDF4 2021 database.

Point Zero Charge (pH_{pzc}) Determination

For pH_{pzc} determination, the procedures were adopted from literature [7,9,32]. Zeolites samples were immersed in 0.01 M KNO_3 solutions adjusted with 0.1 M HNO_3/KOH to obtain pH values of 2, 4, 6, 8, 10, and 12. Mixtures of a ratio of 0.2 % w/v were shaken at 180 rpm for 24 h. Mixtures were vacuum filtered with filter paper #1. Final pH of the filtrate was determined. The pH_{pzc} was determined at the pH value at the plateau of the curve ($pH_f = f(pH_i)$) by plotting the initial pH and final pH.

Batch Adsorption

Standard acetylsalicylic acid solutions (20, 40, 60, 80, 100, 120 ppm) were prepared from a 500 ppm stock solution of acetylsalicylic acid dissolved in 20 % v/v methanol-water solution at pH 7.5. The SMNZs and unmodified zeolites (UZs) were shaken in the standard drug solutions in a ratio of 0.2 % w/v at 180 rpm for 60 min. Mixtures were centrifuged at 14,500 rpm for 5 min. UV absorption measurements of the supernatants were carried out using 96-well microplate reader BMG Labtech FLUOstar Omega at ≈ 280 nm. Data obtained were used to plot the adsorption isotherms, particularly the Langmuir and Freundlich isotherms. The equations for the said isotherms and their linear transformations are indicated in **Table 1**.

Table 1 Adsorption isotherms equation and corresponding variables.

Isotherm	Equation	Variables and constants
Langmuir	Linear: $\frac{C_e}{Q_e} = \frac{1}{Q_{max}} C_e + \frac{1}{Q_{max} K_L}$ (3) Plot:	K_L ($L\ mg^{-1}$) = Langmuir constant, C_0 ($mg\ g^{-1}$) = Initial concentration of the adsorbate, constant Q_e ($mg\ g^{-1}$) = amount of loaded adsorbate,

Isotherm	Equation	Variables and constants
	$Q_e = Q_{max}\dfrac{K_L C_e}{1+K_L C_e}$ (4)	C_e (mg L^{-1}) = concentration of adsorbate in solution at equilibrium; Q_{max} (mg g^{-1}) = highest concentration of adsorbate
Freundlich	Linear: $\ln(Q_e) = \dfrac{1}{n}\ln(C_e) + \ln(K_f)$ (5) Plot: $Q_e = K_f C_e^{\frac{1}{n}}$ (6)	K_f (L mg^{-1}) = Freundlich constant, 1/n = a constant associated with adsorption intensity, Q_e (mg g^{-1}) = amount of loaded adsorbate, C_e (mg L^{-1}) = concentration of adsorbate in solution at equilibrium,

Results and discussion

Confirmation of surfactant functionalization

Natural zeolites are microporous crystalline hydrated aluminosilicates. This characteristic imparts a negative charge on its surface; therefore, suggests a highly hydrophilic surface area [2,7,17,21-23,25,33]. This is well consistent with the observations in **Figures 1(A) - 1(B)** where UZs and Na-Zs suspensions were found to be in the aqueous layer as also demonstrated by Tran *et al.* [23]. In contrary, phase distribution of cationic SMNZs in the hexane-water phase system is localized in the interface between the layers as shown in **Figures 1(C) - 1(F)**. This suggests that SMNZs exhibit dominant hydrophobic surface; therefore, indicating presence of organic component on its surface [2,3,7,18,23,31].

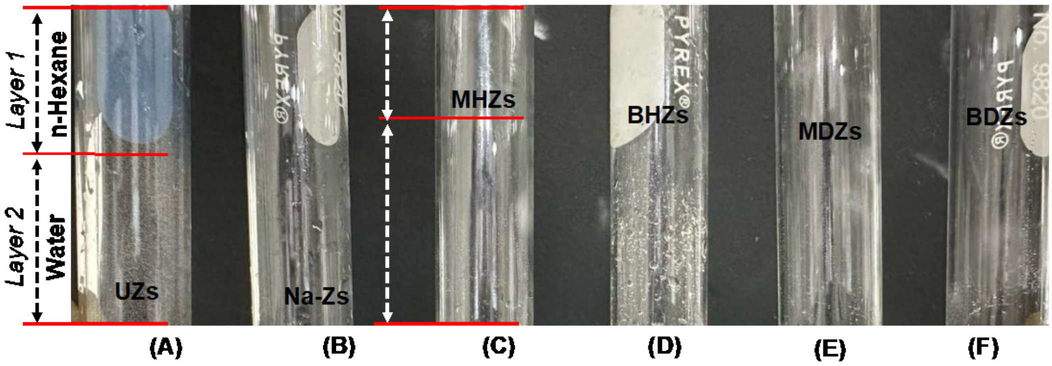

Figure 1 Distribution of zeolites in hexane and water where the turbid region indicates solvent in which the zeolite has a higher affinity to. (A) UZs. (B) Na-saturated Zeolites. (C) Monolayer HDTMA-Br modified Zeolites (MHZs). (D) Bilayer HDTMA-Br Zeolites (BHZs). (E) Monolayer DODA-Br Zeolites (MDZs). (F) Bilayer DODA-Br Zeolites (BDZs).

To further confirm the presence of these organic components at the surface, the FTIR-ATR spectra of the UZs and SMNZs are presented in **Figure 2**. In contrast to UZs, SMNZs have 2 distinct peaks around 2,850 and 2,920 cm^{-1} which are assigned to the symmetric and asymmetric stretching of sp^3 CH peaks of the surfactants. Exclusive presence of CH_2 vibrational bands in the SMNZs is a characteristic of surfactant molecules at the zeolite surface otherwise absent in UZs [7,9,11,14,34,35]. Moreover, the relative intensity among SMNZs increased with the amount of surfactant employed such that more intense signals in bilayer modifications compared to their monolayer counterparts as presented in **Figure 2(A)**. Similarly, this is also observed in comparing HDTMA and DODA modified zeolites (MHZs vs MDZs and BHZs vs BDZs) whereas two-tailed surfactant DODA (18-C) zeolites exhibit stronger signals compared to one-tailed surfactant HDTMA (16-C) zeolites. Nonetheless, both UZs and SMNZs exhibit the typical infrared spectroscopic pattern for silicates. Strong characteristic vibrations of aluminosilicates at 900 - 1,200 cm^{-1} were observed in all samples which are assigned to the T-O stretching attributed to the TO_4 tetrahedra structure of zeolites (T = Si, Al) [2,11,14,34,36,37]. Specifically, a shoulder at 1,220 cm^{-1} and a peak at 1,010 cm^{-1} are from the asymmetric stretching of T-O while the peak at 875 cm^{-1} belongs to the asymmetric stretching of T-O-T. Additionally, low intensity peak at 1,640 cm^{-1} and weak broad vibration at 3,500 cm^{-1} pertain to O-H bending and stretching, respectively. This infers that the aluminosilicate samples are hydrated [7,9,11,14,24,36,37]. These results confirmed the presence of surfactant molecules in SMNZs' surface which explains the acquired hydrophobicity demonstrated in **Figure 1**, and that the functionalization did not impart structural changes in the base zeolite material.

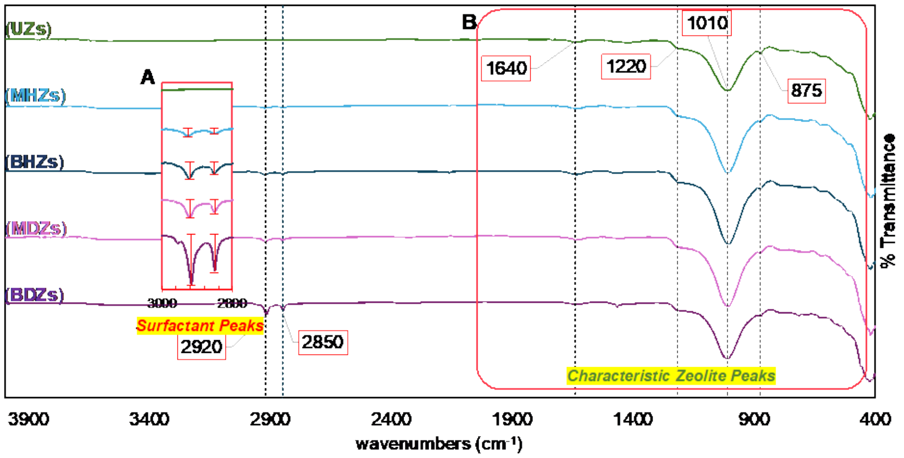

Figure 2 FTIR of zeolite samples. (A) (Inset) distinct sharp peaks of saturated C-H stretching at 2,920 and 2,850 cm^{-1} of SMNZs compared to UZs. (B) Zeolite structural vibrations (TO vibrations at 875, 1,010, and 1,220 cm^{-1}) and OH vibrations at 1,640 and 3,000 - 3,500 cm^{-1}.

To investigate the surface morphology of UZs and SMNZs, SEM images were taken. **Figure 3** shows heterogenous aggregated particles. Both UZs and SMNZs exhibit jagged edges and irregular surface. However, a slightly smoother surface can be observed in all SMNZs (**Figures 3(B)** - **3(E)**) compared to UZs (**Figure 3(A)**) which suggests a change brought about by surfactant-modification. This supports the data from the FTIR that the surface of the zeolite was covered with the surfactants, as well as the hydrophobic behavior observed in **Figure 1**.

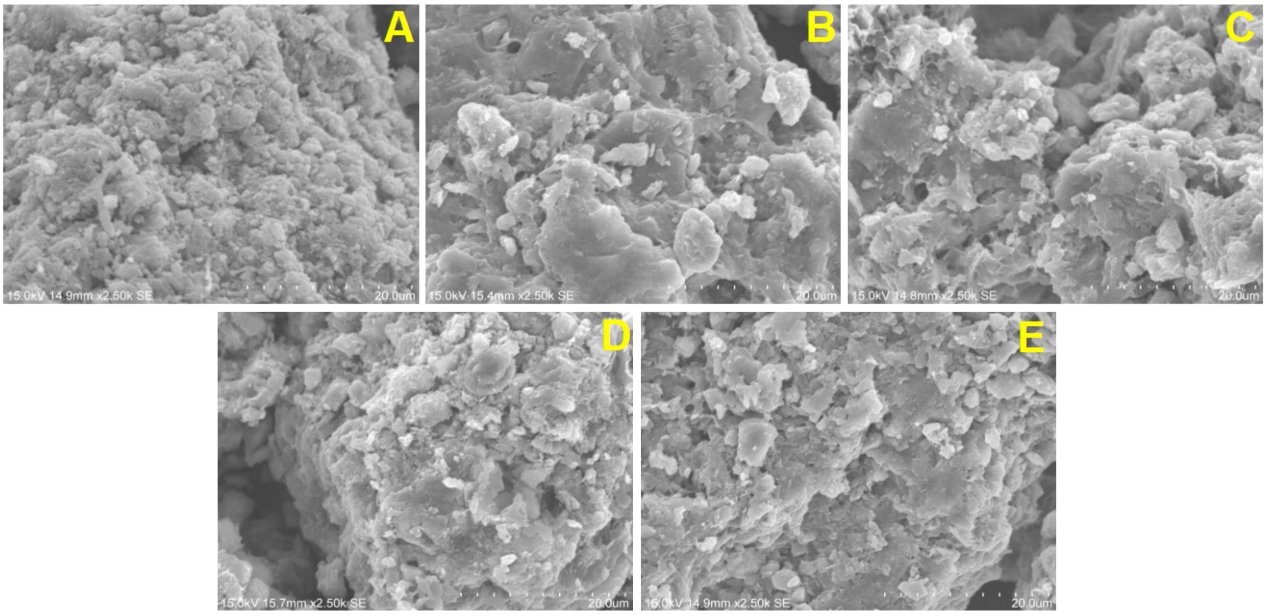

Figure 3 SEM Images at 2500x magnification of (A) UZs, (B) MHZs, (C) BHZs, (D) MDZs, and (E) BDZs.

Table 2 shows the elemental composition of the zeolite surface based on the EDX data. The surface composition of all zeolite samples possesses all the zeolitic structural elements such as Al, Si, O which are typical for any aluminosilicate minerals. Moreover, the presence of inorganic cations such as Na, Mg, K, Ca pertaining to the external exchangeable cations on the zeolite surface was observed. Other cations observed were Fe and Ti. After surfactant functionalization, an increased amount of carbon was evident across all SMNZs compared to UZs. Furthermore, bilayer modified samples (BHZs, BDZs) were found to have higher carbon content on the surface compared to the monolayer samples (MHZs, MDZs). Additionally, zeolites modified with 2 tailed surfactants (BDZs, MDZs) were also found to have higher carbon content compared to their 1 tailed counterpart (BHZs, MHZs). This trend reinforces the similar observations in the FTIR data of SMNZs.

Table 2 Element Wt.% of zeolitic samples surface across 6 different sampling areas presented as mean ± SD. (Red are signals attributable to the surfactant modification while Green are elemental characteristics of zeolite).

Elements	UZs	MHZs	BHZs	MDZs	BDZs
C	-	4.50 ± 0.65	7.19 ± 1.96	5.51 ± 1.63	13.16 ± 2.10
O	37.58 ± 0.55	40.51 ± 2.19	38.41 ± 2.53	39.69 ± 2.69	35.15 ± 2.23
Na	1.56 ± 0.21	1.60 ± 0.15	1.36 ± 0.24	1.48 ± 0.27	1.13 ± 0.25
Mg	0.64 ± 0.17	0.47 ± 0.10	0.49 ± 0.15	0.51 ± 0.10	0.48 ± 0.15
Al	6.98 ± 0.27	7.02 ± 0.41	7.09 ± 0.33	6.84 ± 0.18	7.14 ± 0.34
Si	36.94 ± 0.40	37.41 ± 1.82	35.73 ± 2.55	34.54 ± 3.16	32.32 ± 1.30
K	1.09 ± 0.18	0.88 ± 0.16	0.68 ± 0.17	3.96 ± 3.31	0.75 ± 0.16
Ca	9.05 ± 0.22	3.10 ± 0.36	2.79 ± 0.46	2.82 ± 2.72	3.46 ± 1.19
Ti	0.22 ± 0.12	0.54 ± 0.17	1.30 ± 1.66	2.58 ± 2.31	0.84 ± 0.39
Fe	4.94 ± 0.41	3.81 ± 0.88	4.29 ± 2.84	4.16 ± 0.92	5.26 ± 1.31

Figure 4 shows the DSC data of UZs and SMNZs. A broad endothermic peak around 75 to 200 °C was observed across all the samples. This can be attributed to zeolite dehydration of loosely bound H_2O detected as weak vibrational band in 3,000 - 3,500 cm^{-1} in the FTIR-ATR [10,13,26,38]. Although no distinct variations were observed across the thermograms, we suspect that the surfactant desorption and decomposition may overlap with the dehydration. Olegario *et al.* [38] reported that in temperatures 103.8 to 660 °C, decomposition of tightly bound H_2O or zeolitic H_2O occurs. To elucidate further these thermal variations especially at higher temperatures, Thermogravimetric - Differential Thermal Analysis was employed.

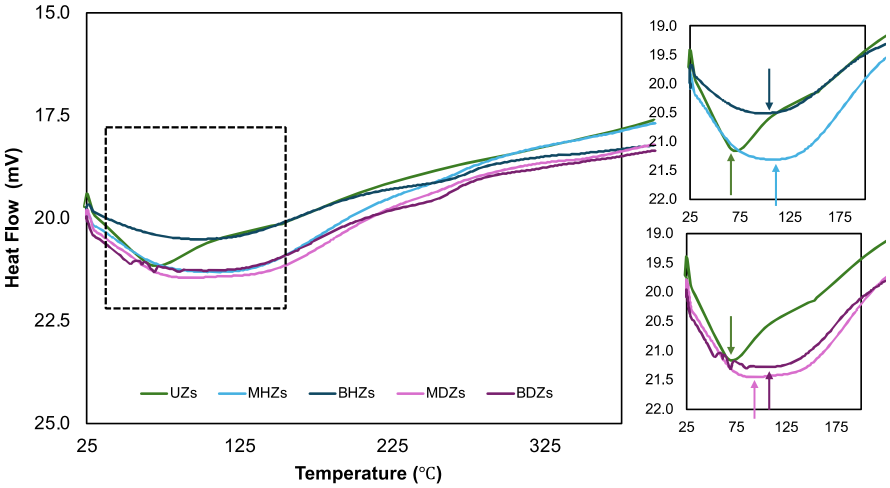

Figure 4 DSC thermograms of zeolite samples. Endothermic peaks attributed to dehydration are observed in all samples. However, early onset of dehydration at lower temperatures was observed for UZs compared to SMNZs.

In agreement with **Figure 4**, an endothermic peak attributed to dehydration in DTA-DTG was redemonstrated in **Figure 5(A)**. for both UZs and Na-Zs. Moreover, their TG thermograms (**Figures 5(B)** - **5(C)**) were similar and their maximum weight loss was recorded as 16 and 17 % at 699 and 696 °C, respectively. However, a weak endothermic reaction around 500 °C in UZs was observed whereas absent in Na-Z. This is suspected from the decomposition of residues in UZs that are otherwise absent in Na-Zs after exhaustive zeolite cleaning and Na-saturation [2,7,11,24,38]. Across all the samples, initial weight losses are attributed to the continuous dehydration [11,24,26,38,39]. As far as SMNZs are concerned especially in 200 - 800 °C, combustion of surfactants overlaps with zeolitic water desorption [9,10,40] as demonstrated by **Figure 5(A)**. which results to larger endothermic peaks in SMNZs compared to UZs and Na-Zs. It can be deduced that higher energy requirements are needed to decompose the organic modification [2,3,7]. Additionally, higher maximum weight loss of BHZs and BDZs recorded as 20 and 24 % account for the decomposition of surfactants [3,7,19,34,39,41]. Moreover, higher mass loss observed in BDZs coincides with the higher surface carbon content reported in EDX. This suggests that DODA modification imparts a larger amount of organic layer which intuitively corresponds to the longer two-tailed carbon chains of the surfactant compared to HDTMA. In the interest to examine the number of organic layers, TGA was also used to assess the surfactant loading (**Figures 5(B)** - **5(C)**) [13,23,40-43]. The first recorded mass loss peak, which occurred at 261 and 288 °C for BHZs and BDZs, was attributed to the weakly bound bilayer of surfactant or non-adsorbed surfactants [42]. Furthermore, the second recorded mass loss peak, which occurred 392 and 360 °C, was attributed to the monolayer of the surfactants. This temperature-specific layer decomposition was also observed by Guan (2010) and reported by Reeve (2018) [13,42]. Thermal data concur with the earlier findings from other characterizations and further elucidated the bilayer modifications.

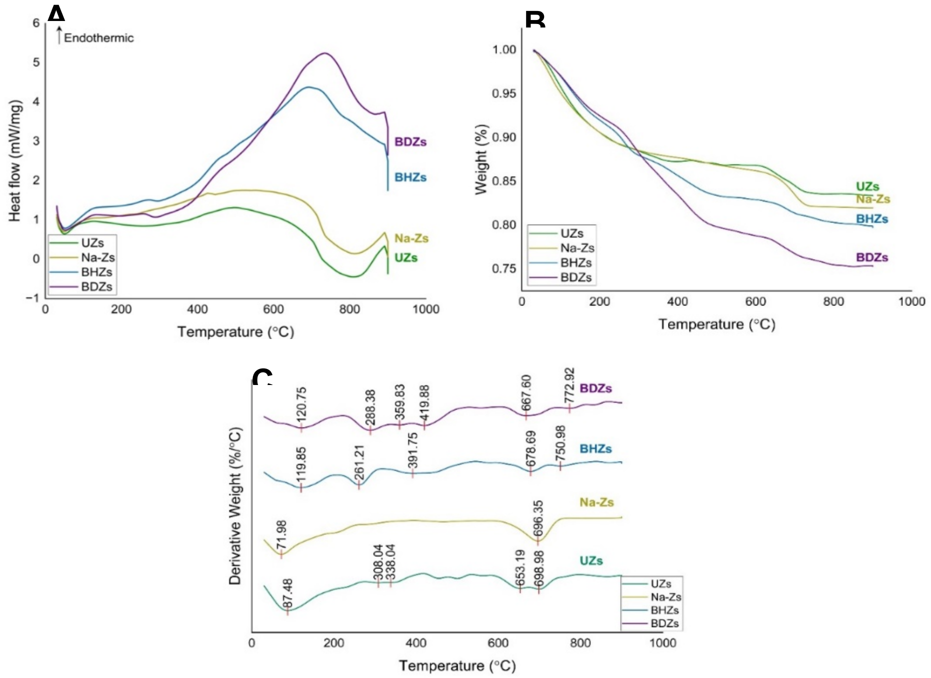

Figure 5 DTA-DTG profile of zeolites. (A) Differential thermal analysis, (B) Thermogravimetric, (TG) Thermograms (C) Differential thermogravimetric (DTG) thermograms.

Previous characterizations have demonstrated the presence of the organic layers yet its implication on the surface activity of the adsorbent has not been extensively discussed. Zeta potential corresponds to the surface potential of the material, and it changes on the surfactant loading at the surface as shown by **Figure 6**. Supposedly, when the surfactant concentration used is equal to 100 % of ECEC, the zeta potential should be close to zero to mark the enhanced hydrophobicity of the surface and the masking of zeolite's negative charge on the surface. Similarly, when the surfactant concentration is equal to 200 % ECEC, the surfactant bilayer should impart a more positive measurement due to exposed amino groups in the bilayer [7,9,13,17,28,39,44]. As demonstrated in **Figure 6**, zeta potential of 100 % of ECEC surfactant modifications are relatively more positive compared to UZs. This suggests that at surfactant modifications of 100 % ECEC, surfactant molecules can cover significant surface area of the zeolite [7,9,17,28,45]. On the other hand, zeta potential of 200 % of ECEC surfactant modifications are all greater than zero. This implies the formation of either bilayers or patchy bilayers [9,13,17,45]. Results in the monolayer modification express that although these quaternary ammonium possess different functional groups, their similar effect on the zeta potential at < 100 % of ECEC suggest that they are similarly positioned in the zeolite surface as reasoned by Smiljinac (2022). Interestingly, zeta potential also underscores the stability of the colloidal suspensions [46,47]. Bilayer modifications result to an enhanced positively charged character of the surface as reflected by the positive zeta potential [2,3,7,39]. As a result, particles highly repel each other to resist flocculation and retain the colloidal stability [46,47]. This offers significant insights in adsorption optimization since a highly dispersed adsorbent suspension maximize surfaces area for adsorption. Nonetheless, the findings reaffirm with FTIR-ATR, EDX, DTA-DTG data in describing the changes brought by the type and amount of surfactant employed.

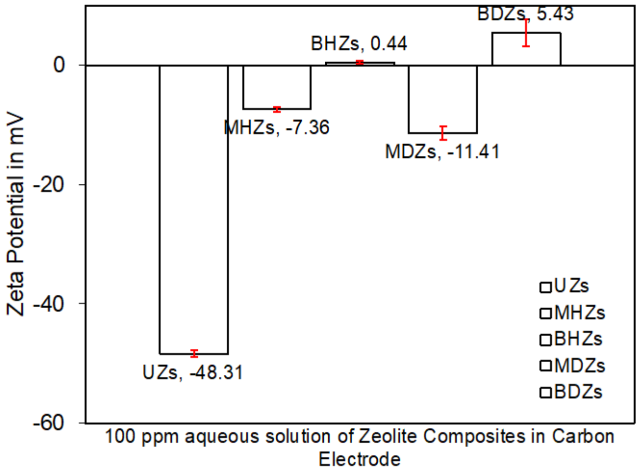

Figure 6 Zeta potential of zeolite samples. UZs, MHZs, and MDZs exhibits negative zeta potential compared to BHZs and BDZs.

Diffractograms on **Figure 7** reveal that the natural zeolite possesses characteristic peaks for mordenite (PDF 00-060-0846) and heulandite (PDF 00-053-1176). These specific class of zeolites have demonstrated adsorptive properties based on previous literatures [48,49]. It was observed that SMNZs have similar diffractograms with UZs. This demonstrates that the crystalline structure of UZs was unchanged by the surfactant modification. Therefore, this suggests that the surfactant modification primarily occurs in the zeolite surface as seen previously in literature [19,31,35,50,51].

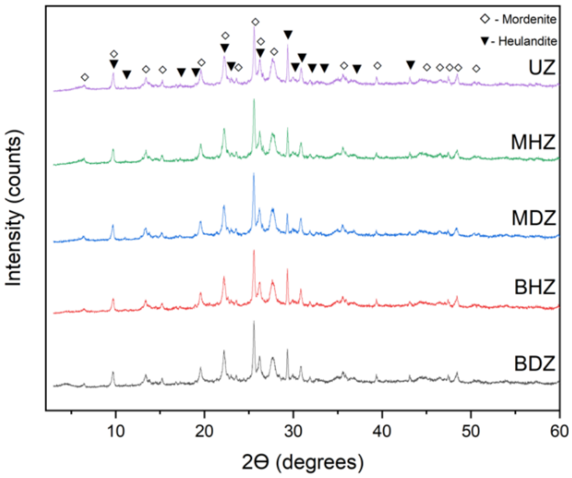

Figure 7 X-ray Diffractograms of UZs and SMNZs (H = heulandite and M = mordenite).

Although zeta potential measurements can capture the surface charges of the adsorbent, these parameters are sensitive to the pH of the solution. To optimize the removal efficacy of the adsorbents, understanding the physicochemical properties of the material such as polarity and charge distribution is significant [7,52]. The point-zero-charge (pH_{PZC}) determines the state of the surface of dispersed particles at the solid-electrolyte solution interface. Specifically, pH_{PZC} is the pH at which the surface has a net zero charge [7]. At a certain range of pH, the adsorbent acts as a buffer by either associating or dissociating hydroxyl groups with the solution. From **Figures 8(A) - 8(D)**, similar shapes of $pH_f = f(pH_I)$ curve and plateau among all the samples suggest similar buffering and amphoteric behavior especially at $4 < pH < 10$. Moreover, approximately close pH_{PZC} values of SMNZs and UZs agrees with the findings of Smiljanic and Dakovic [3,34]. They rationalize this outcome that

SMNZs possess similar surface functional groups with similar acid and basic characteristics as the base materials. As far as the adsorption is concerned, batch experiments for acetylsalicylic acid were conducted at pH ≈ 7.5. PZC data implicates that the majority surfaces of SMNZs and UZs are uncharged at pH 7.5; therefore, suggesting that the adsorption at these conditions must be largely influenced by hydrophobic interactions.

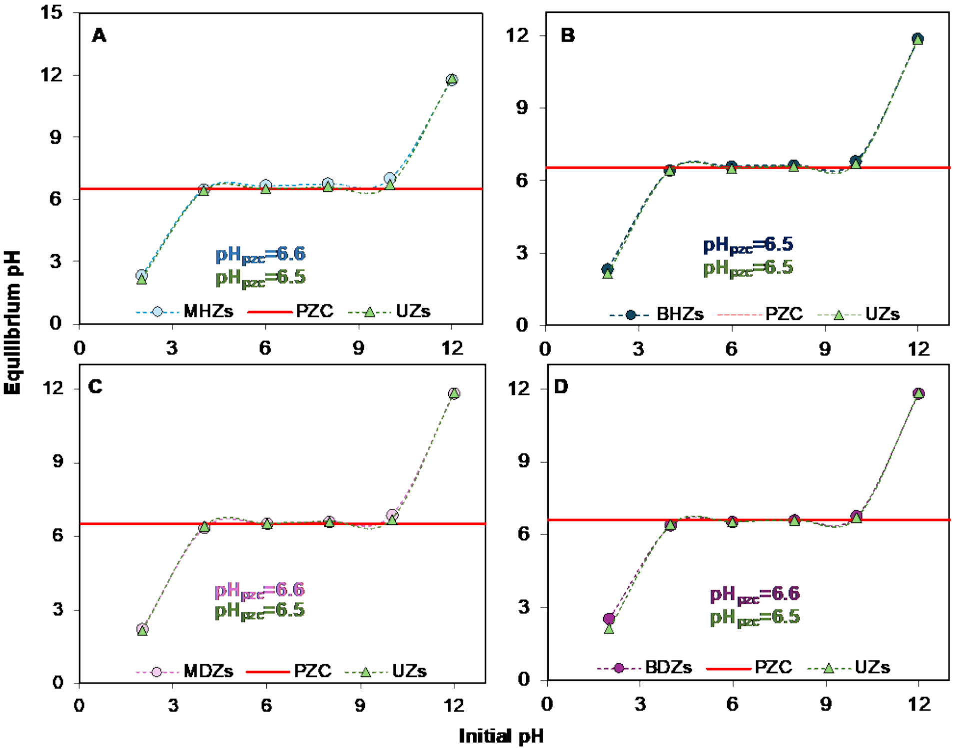

Figure 8 Average $pH_f = f(pH_I)$ plots of Zeolite Composites at 0.01 M KNO_3 solutions at pH 2, 4, 6, 8, 10, 12. (A) UZs vs MHZs (B) UZs vs BHZs (C) UZs vs MDZs (D) UZs vs BDZs.

Ultimately, the FTIR-ATR, SEM-EDX, DSC, DG-TGA, and Zeta Potential have thoroughly demonstrated the surfactant modification. On the other hand, XRD patterns strongly established that the modification has no relevant implications on the structural integrity of the sample. Additionally, Zeta potential and PZC measurements provided us with crucial considerations concerning the stability and surface charge distribution of the adsorbent.

Batch adsorption of acetylsalicylic acid

All SMNZs were able to reduce the concentrations of acetylsalicylic acid. **Figure 9** shows the percent remaining concentration of acetylsalicylic acid at 20 ppm. Importantly, the percent removal of UZs, MHZs, BHZs, MDZs, and BDZs were 26.0 ± 4.7, 37.4 ± 3.9, 43.4 ± 4.3, 36.9 ± 6.7, 57.0 ± 7.5 percent, respectively. This shows a maximum of about 119 % improvement in percent removal brought about by surfactant modification.

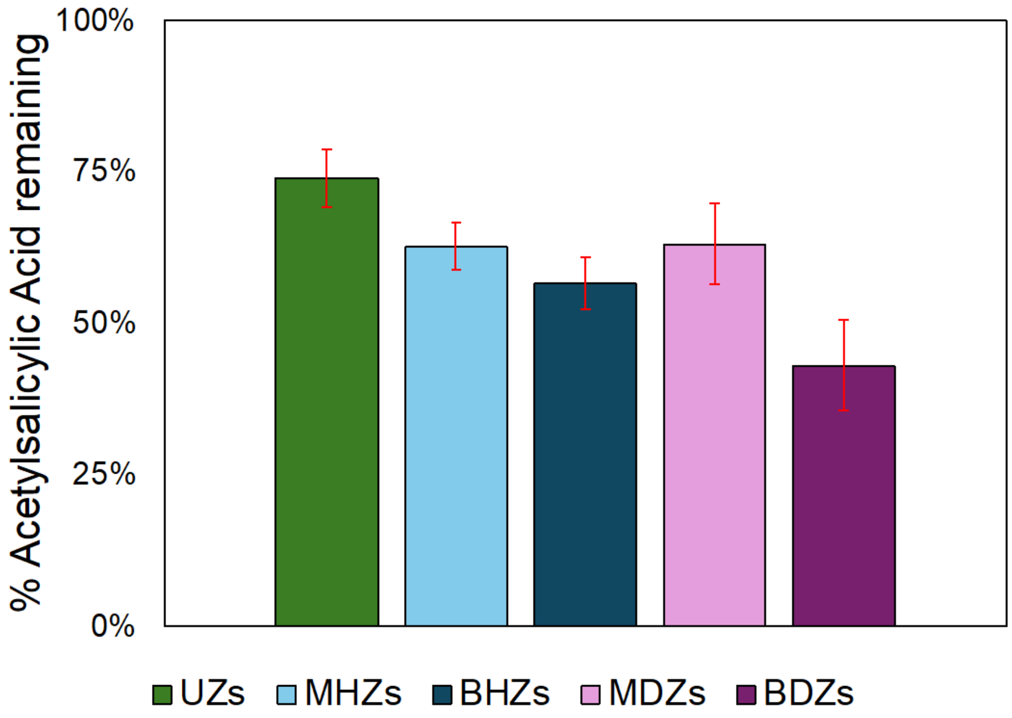

Figure 9 Remaining acetylsalicylic acid (%) from 20 ppm acetylsalicylic acid solution after shaking for 60 min at 180 rpm.

The isotherms of acetylsalicylic acid adsorption on UZs and SMNZs are illustrated in **Figure 10**. Data demonstrates that acetylsalicylic acid adsorption increases with the initial drug concentration (C_e). All SMNZs demonstrated higher adsorption capacity compared to UZs. Noticeably, a higher degree of adsorption is observed in bilayer modifications compared to their monolayer counterparts. This suggests that the concentration of surfactant is a key parameter in optimizing the adsorption capacity of the SMNZs [2,7,9]. In the bilayer modified zeolites, the exposed quaternary ammonium of the bilayer interacts with the carboxylate group of acetylsalicylic acid via anion exchange mechanism with bromide counterions, and electrostatic interactions as illustrated in **Figure 11** [2,3,7,9]. Although acetylsalicylic acid exists in the anionic form at pH > 4, the compound remains relatively nonpolar. This also permits hydrophobic interaction of acetylsalicylic acid in the bilayer's hydrocarbon chains.

In a similar experiment by Choi and Shin, salicylic acid, as acetylsalicylic acid metabolite, adsorbs onto HDTMA-modified zeolite occurs by coulombic interaction with the positively charged head of the surfactant and that the benzene ring of salicylic acid can be reoriented within the monolayer/bilayer and subsequently stabilized by the 16-C chain of HDTMA [6]. Additionally, Davila-Estrada (2018) and Krajisnik (2010, 2011) suggested that the occurrence of hydrophobic partitioning [34,41,53] where adsorbed organic molecules dissolves in the organic layer formed by the alkyl chains of the surfactants. We suspect that the hydrophobic partitioning may contribute to the adsorption of acetylsalicylic acid on the monolayer SMNZs. This implies that the presence of anion exchange mechanism in bilayer samples, that is otherwise absent in monolayer samples, enhances the acetylsalicylic acid adsorption.

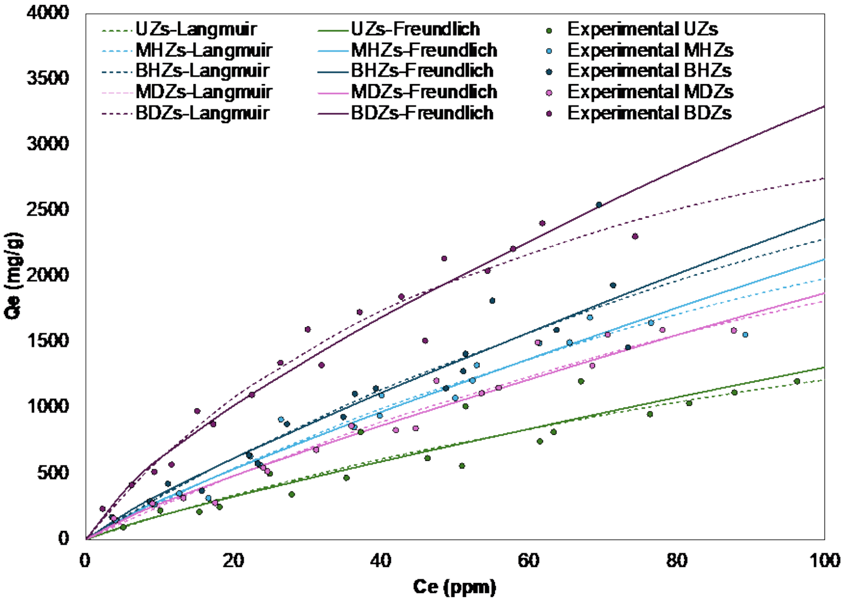

Figure 10 Langmuir and freundlich non-linear adsorption isotherm models for natural zeolite samples and experimental data points across 3 trials.

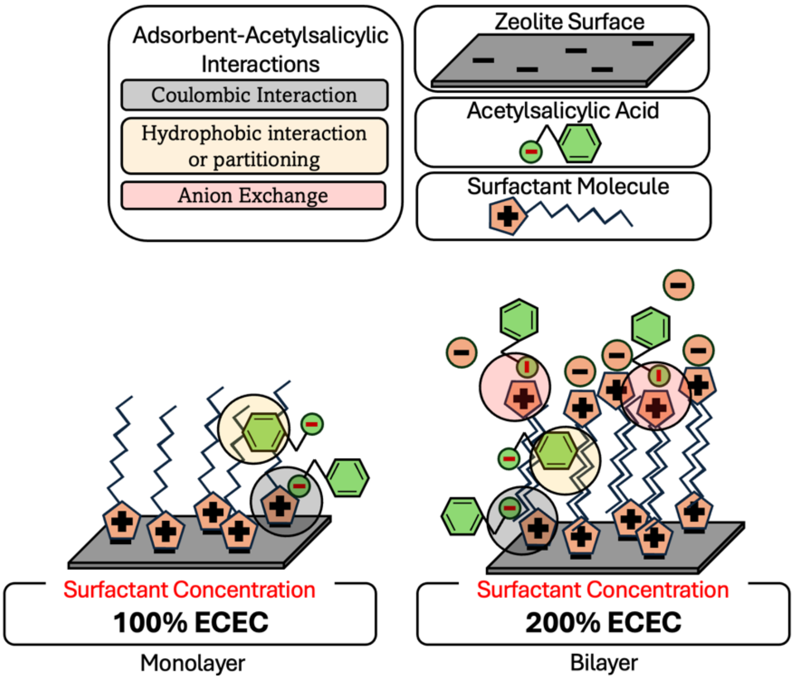

Figure 11 Suggested acetylsalicylic acid and SMNZs surface interaction.

To quantitate the behavior of the adsorption, coefficient of determination of the isotherm models are shown in **Figure 12**. It shows that the degree of linearity is best observed in Freundlich isotherms compared to Langmuir isotherms. This suggests that the SMNZs and UZs possess heterogenous adsorption sites where stronger binding sites is occupied first and subsequent adsorption energy for the succeeding bindings exponentially decreases [19,26,41,54]. We suspect that the naturally occurring irregular shaped zeolites implicates heterogenous surface binding sites as reflected in the SEM Images. Studies on surfactant modified clinoptilolite [7,9,19,26,41,54], chabazite [26], phillipsite [2,9-11], and montmorillonite [6,20,33] have also been demonstrated good-fitting for Freundlich isotherms for adsorption of their targeted pharmaceuticals. As shown in the linear transformations in **Figure 13**, Freundlich isotherms have higher R^2

(**Figures 13(D) - 13(F)**) compared to Langmuir Isotherms (**Figures 13(A) - 13(C)**) across all trials. This reinforces that the Freundlich isotherm model describe the adsorption better compared to Langmuir.

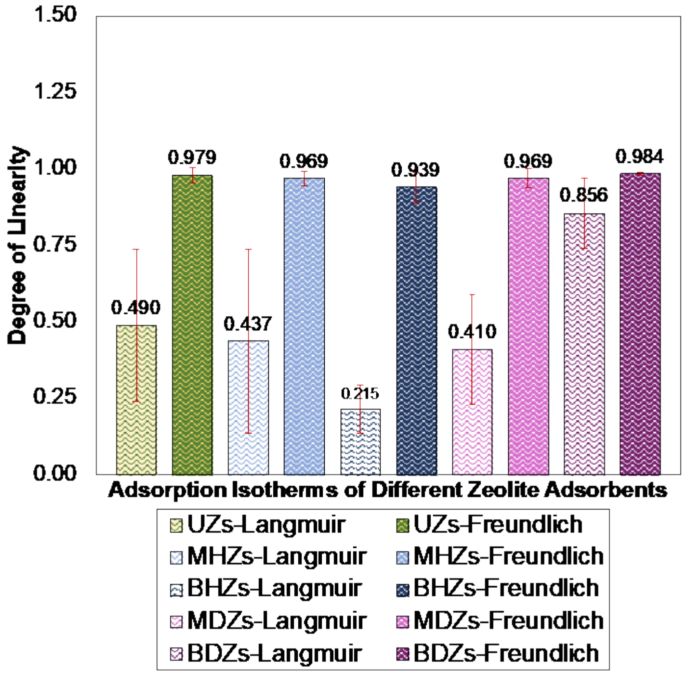

Figure 12 Degree of linearity of isotherm models and their corresponding standard error from the mean from 3 trials.

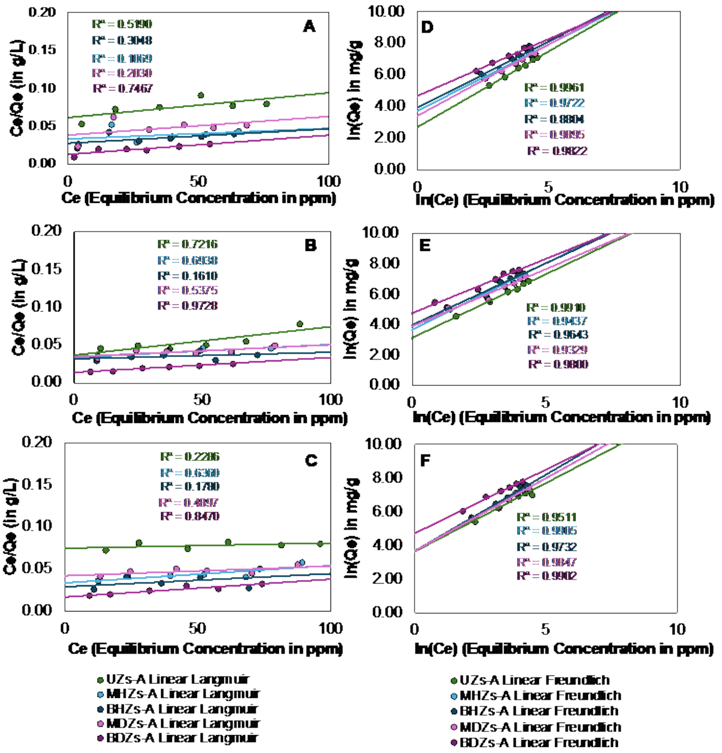

Figure 13 Linear transformations of experimental data for langmuir and freundlich isotherm models fitting for 3 trials. (A) - (C). Langmuir isotherm fitting for trials 1 - 3 (D) - (F). Freundlich isotherm fitting for trials 1 - 3. *R^2 refers to the coefficient of determination.*

Using the linear transformations, key parameters from Freundlich isotherms were obtained as shown in **Figure 14**. Among all the adsorbents, BDZs displayed the highest affinity (113.34 ± 6.73 with p-value < 0.05 compared to all adsorbents) and relatively the most favorable adsorption for acetylsalicylic acid among all adsorbents as shown in **Figure 14(B)**. This highlights the role of two-tailed surfactant DODA and bilayer architecture as key elements for enhanced acetylsalicylic acid adsorption on natural zeolites. **Table 3** shows that BDZs' affinity (K_f) towards acetylsalicylic acid is superior to other materials from previous studies. With this promising result, it is worthwhile to explore further the bilayer architecture of DODA-modified zeolite and apply it to other drugs and pollutants of emerging concern.

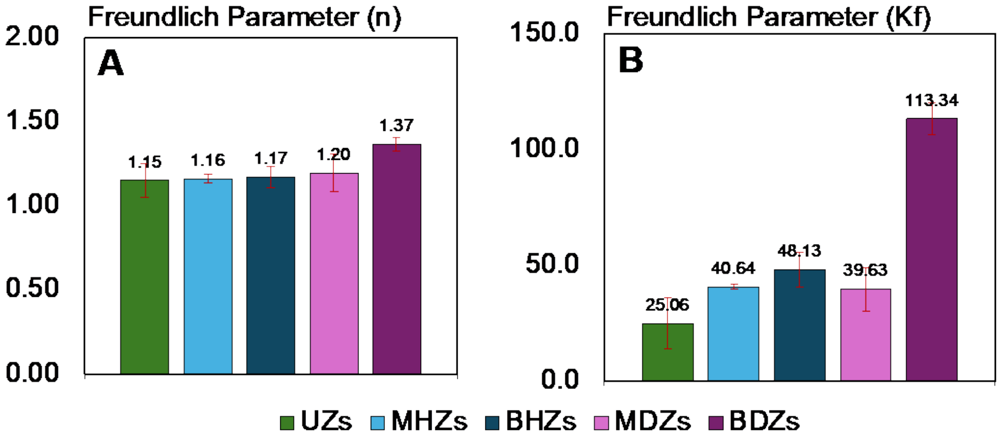

Figure 14 Determined Freundlich parameters of acetylsalicylic acid adsorption using SMNZs and UZs. (A) Order of Adsorption (n) (B) Affinity (K_f).

Table 3 Freundlich parameters of acetylsalicylic acid adsorption by different adsorbents.

Parameters	**Adsorbents from other literature**				**BDZs (This study)**
	Crosslinked polymer network [55]	**Biochar [56]**	**Nanocomposites [57]**	**Activated Carbon [58]**	
K_f	87.08	3.60	2.87	5.40	113.34
n	5.631	3.33	2.1	1.75	1.37
R^2	0.9997	0.9483	0.998	0.9763	0.984

Conclusions

Surfactant modification of natural zeolites using HDTMA and DODA was successfully demonstrated. Presence of surfactant layers on the surface of the zeolites was confirmed using TGA, SEM images, FTIR, EDX, and Zeta Potential measurements. The FTIR data highlights the presence of characteristic peaks of the surfactants in SMNZs. Elemental analysis using EDX supports the idea of surfactant modification at the surface. XRD data, on the other hand, showed that the zeolite phases present are mordenite and heulandite and that the crystallinity of the zeolite was preserved after modification. Batch adsorption experiments of SMNZs showed enhanced removal of acetylsalicylic acid compared to UZs up to a maximum of about 119 % improvement. This suggests that anion exchange, electrostatic, and hydrophobic interactions between the zeolite and acetylsalicylic acid brought about by surfactant-modification improve the adsorption of the acetylsalicylic acid on the surface of the zeolites. The adsorption behavior was described using the Freundlich isotherm. Specifically, a high K_f value of 113.34 or higher affinity observed in BDZs suggests the role of two-tailed DODA. This study highlights the promising potential of BDZs towards the removal of emerging pollutants like acetylsalicylic acid for wastewater treatment. To further investigate its adsorption performance, it is recommended to explore effects of pH, and temperature; and determine its desorption properties before investigating further its role in an actual industrial-scale wastewater treatment facility.

Acknowledgements

The authors would like to acknowledge DOST-PCIEERD for the financial support under the HRDP Balik Saliksik Program (PCIEERD Project No. 1211425). Mr. Araneta and Mr. Seagan would also like to acknowledge DOST-SEI for its financial support. The authors would also like to acknowledge the Center for Advanced New Materials, Engineering, and Emerging Technologies of the University of San Agustin, Philippines for the DLS analysis.

References

[1] TAD Beek, F Weber, A Bergmann, S Hickmann, I Ebert, A Hein and A Kuster. Pharmaceuticals in the environment--global occurrences and perspectives. *Environmental Toxicology and Chemistry* 2016; **35(4)**, 823-835.

[2] D Smiljanic, BD Gennaro, F Izzo, A Langella, A Dakovic, C Germinario, GE Rottinghaus, M Spasojevic and M Mercurio. Removal of emerging contaminants from water by zeolite-rich composites: A first approach aiming at diclofenac and ketoprofen. *Microporous and Mesoporous Materials* 2020; **298**, 110057.

[3] D Smiljanic, BD Gennaro, A Dakovic, B Galzerano, C Germinario, F Izzo, GE Rottinghaus and A Langella. Removal of non-steroidal anti-inflammatory drugs from water by zeolite-rich composites: The interference of inorganic anions on the ibuprofen and naproxen adsorption. *Journal of Environmental Management* 2021; **286**, 112168.

[4] M Parolini. Toxicity of the non-steroidal anti-inflammatory drugs (NSAIDs) acetylsalicylic acid, paracetamol, diclofenac, ibuprofen and naproxen towards freshwater invertebrates: A Review. *Science of The Total Environment* 2020; **740**, 140043.

[5] K Swiacka, A Michnowska, J Maculewicz, M Caban and K Smolarz. Toxic effects of NSAIDs in non-target species: A review from the perspective of the aquatic environment. *Environmental Pollution* 2021; **273**, 115891.

[6] J Choi and WS Shin. Removal of salicylic and ibuprofen by hexadecyltrimethylammonium-modified montmorillonite and zeolite. *Minerals* 2020; **10(10)**, 898.

[7] D Smiljanic, A Dakovic, M Obradovic, M Ozegovic, F Izzo, C Germinario and BD Gennaro. Application of surfactant modified natural zeolites for the removal of salicylic acid-a contaminant of emerging concern. *Materials* 2021; **14(24)**, 7728.

[8] S Aydin, ME Aydin and A Ulvi. Monitoring the release of anti-inflammatory and analgesic pharmaceuticals in the receiving environment. *Environmental Science and Pollution Research* 2019; **26(36)**, 36887-36902.

[9] D Smiljanic, A Dakovic, M Obradovic, M Ozegovic, M Markovic, GE Rottinghaus and BD Gennaro. Influence of the type and the amount of surfactant in phillipsite on adsorption of diclofenac sodium. *Catalysts* 2022; **13(1)**, 71.

[10] F Izzo, M Mercurio, BD Gennaro, P Aprea, P Cappelletti, A Dakovic, C Germinario, C Grifa, D Smiljanic and A Langella. Surface modified natural zeolites (SMNZs) as nanocomposite versatile materials for health and environment. *Colloids and Surfaces B: Biointerfaces* 2019; **182**, 110380.

[11] BD Gennaro, P Aprea, B Liguori, B Galzerano, A Peluso and D Caputo. Zeolite-rich composite materials for environmental remediation: arsenic removal from water. *Applied Sciences* 2020; **10(19)**, 6939.

[12] E Perez-Botella, S Valencia and F Rey. Zeolites in adsorption processes: State of the art and future prospects. *Chemical Reviews* 2022; **122(24)**, 17647-17695.

[13] PJ Reeve and HJ Fallowfield. Natural and surfactant modified zeolites: A review of their applications for water remediation with a focus on surfactant desorption and toxicity towards microorganisms. *Journal of Environmental Management* 2018; **205**, 253-261.

[14] D Bhardwaj, M Sharma, P Sharma and R Tomar. Synthesis and surfactant modification of clinoptilolite and montmorillonite for the removal of nitrate and preparation of slow release nitrogen fertilizer. *Journal of Hazardous Materials* 2012; **227-228**, 292-300.

[15] T Lohar, A Kumbhar, A Patil, S Kamat and R Salunkhe. Synthesis and characterization of new quaternary ammonium surfactant [C18-Dabco] [Br] and its catalytic application in the synthesis of spirocarbocycles under ultrasonic condition. *Research on Chemical Intermediates* 2019; **45(3)**, 1639-1651.

[16] R Nodehi, H Shayesteh and AR Kelishami. Enhanced adsorption of congo red using cationic surfactant functionalized zeolite particles. *Microchemical Journal* 2020; **153**, 104281.

[17] RE Apreutesei, C Catrinescu and C Teodosiu. Surfactant-modified natural zeolites for environmental applications in water purification. *Environmental Engineering and Management Journal* 2008; **7(2)**, 149-161.

[18] A Torabian, H Kazemian, L Seifi, GN Bidhendi, AA Azimi and SK Ghadiri. Removal of petroleum aromatic hydrocarbons by surfactant-modified natural zeolite: The effect of surfactant. *CLEAN - Soil, Air, Water* 2010; **38(1)**, 77-83.

[19] M Davila-Estrada, JJ Ramirez-Garcia, MC Diaz-Nava and M Solache-Rios. Sorption of 17α-ethinylestradiol by surfactant-modified zeolite-rich tuff from aqueous solutions. *Water Air & Soil Pollut* 2016; **227(5)**, 157.

[20] G Wang, Y Miao, Z Sun and S Zheng. Simultaneous adsorption of aflatoxin b1 and zearalenone by mono- and di-alkyl cationic surfactants modified montmorillonites. *Journal of Colloid and Interface Science* 2018; **511,** 67-76.

[21] SL Hailu, BU Nair, M Redi-Abshiro, I Diaz and M Tessema. Preparation and characterization of cationic surfactant modified zeolite adsorbent material for adsorption of organic and inorganic industrial pollutants. *Journal of Environmental Chemical Engineering* 2017; **5(4)**, 3319-3329.

[22] J Shi, Z Yang, H Dai, X Lu, L Peng, X Tan, L Shi and R Fahim. Preparation and application of modified zeolites as adsorbents in wastewater treatment. *Water Science & Technology* 2018; **2017(3)**, 621-635.

[23] H Tran, P Viet and H Chao. Surfactant modified zeolite as amphiphilic and dual-electronic adsorbent for removal of cationic and oxyanionic metal ions and organic compounds. *Ecotoxicology and Environmental Safety* 2018; **147**, 55-63.

[24] BD Gennaro, L Catalanotti, RS Bowman and M Mercurio. Anion exchange selectivity of surfactant modified clinoptilolite-rich tuff for environmental remediation. *Journal of Colloid and Interface Science* 2014; **430**, 178-183.

[25] P Cappelletti, A Colella, A Langella, M Mercurio, L Catalanotti, V Monetti and BD Gennaro. Use of surface modified natural zeolite (SMNZ) in pharmaceutical preparations part 1. mineralogical and technological characterization of some industrial zeolite-rich rocks. *Microporous and Mesoporous Materials* 2017; **250**, 232-244.

[26] F Izzo, A Langella, BD Gennaro, C Germinario, C Grifa, C Rispoli and M Mercurio. Chabazite from campanian ignimbrite tuff as a potential and sustainable remediation agent for the removal of emerging contaminants from water. *Sustainability* 2022; **14(2)**, 725.

[27] W Lutz. Zeolite Y: Synthesis, modification, and properties-a case revisited. *Advances in Materials Science and Engineering* 2014; **2014**, 724248.

[28] RS Bowman. Applications of surfactant-modified zeolites to environmental remediation. *Microporous and Mesoporous Materials* 2003; **61(1-3)**, 43-56.

[29] F Morante-Carballo, N Montalvan-Burbano, P Carrion-Mero and N Espinoza-Santos. Cation exchange of natural zeolites: Worldwide research. *Sustainability* 2021; **13(14)**, 7751.

[30] V Jovanovic, V Dondur, L Damjanovic, J Zakrzewska and Tomasevic-Canovic. Improved materials for environmental application: surfactant-modified zeolites. *Maaterials Science Forun* 2006; **518**, 223-228.

[31] N Mirzaei, M Hadi, M Gholami, RF Fard and MS Aminabad. Sorption of acid dye by surfactant modificated natural zeolites. *Journal of the Taiwan Institute of Chemical Engineers* 2016; **59**, 186-194.

[32] S Beninati, D Semeraro and M Mastragostino. Adsorption of paracetamol and acetylsalicylic acid onto commercial activated carbons. *Adsorption Science & Technology* 2008; **26(9)**, 721-734.

[33] S Wang and Y Peng. Natural zeolites as effective adsorbents in water and wastewater treatment. *Chemical Engineering Journal* 2010; **156(1)**, 11-24.

[34] D Krajisnik, M Milojevic, A Malenovic, A Dakovic, S Ibric, S Savic, V Dondur, S Matijasevic, A Radulovic, R Daniels and J Milic. Cationic surfactants-modified natural zeolites: Improvement of the excipients functionality. *Drug Development and Industrial Pharmacy* 2010; **36(10)**, 1215-1224.

[35] D Bhardwaj, P Sharma, M Sharma and R Tomar. Surfactant modified tectosilicates and phyllosilicates for 2,4-D removal and slow release formulation. *RSC Advances* 2014; **4(9)**, 4504-4514.

[36] BD Gennaro, M Mercurio, P Cappelletti, L Catalanotti, A Dakovic, AD Bonis, C Grifa, F Izzo, M Krakovic, V Monetti aand A Langella. Use of surface modified natural zeolite (smnz) in pharmaceutical preparations. part 2. a new approach for a fast functionalization of zeolite-rich carriers. *Microporous and Mesoporous Materials* 2016; **235**, 42-49.

[37] T Bajda and Z Kłapyta. Sorption of chromate by clinoptilolite modified with alkylammonium surfactants. *Mineralogia* 2006; **37(2)**, 93-98.

[38] E Olegario, CM Pelicano, JC Felizco and H Mendoza. Thermal stability and heavy metal (As^{5+}, Cu^{2+}, Ni^{2+}, Pb^{2+} and Zn^{2+}) Ions uptake of the natural zeolites from the philippines. *Materials Research Express* 2019; **6(8)**, 085204.

[39] H Aloulou, A Ghorbel, W Aloulou, RB Amar and S Khemakhem. Removal of fluoride ions (F^-) from aqueous solutions using modified turkish zeolite with quaternary ammonium. *Environmental Technology* 2021; **42(9)**, 1353-1365.

[40] R Leyva-Ramos, A Jacobo-Azuara, PE Diaz-Flores, RM Guerrero-Coronado, J Mendoza-Barron and MS Berber-Mendoza. Adsorption of chromium(VI) from an aqueous solution on a surfactant-modified zeolite. *Colloids and Surfaces A: Physicochemical and Engineering Aspects* 2008; **330(1)**, 35-41.

[41] D Krajisnik, A Dakovic, M Milojevic, A Malenovic, M Kragovic, DB Bogdanovic, V Dondur and J Milic. Properties of diclofenac sodium sorption onto natural zeolite modified with cetylpyridinium chloride. *Colloids and Surfaces B: Biointerfaces* 2011; **83(1)**, 165-172.

[42] H Guan, E Bestland, C Zhu, H Zhu, D Albertsdottir, J Hutson, CT Simmons, M Ginic-Markovic, X Tao and AV Ellis. Variation in performance of surfactant loading and resulting nitrate removal among four selected natural zeolites. *Journal of Hazardous Materials* 2010; **183(1-3)**, 616-621.

[43] AJR Capistrano, RJD Labadan, JEB Viernes, EM Aragua, RN Palac and RO Arazo. Ibuprofen removal using activated carbon from acid-modified acacia sawdust. *Energy Ecology Environment* 2023; **8**, 101-112.

[44] MM Hussein, KM Khader and SM Musleh. Characterization of raw zeolite and surfactant-modified zeolite and their use in removal of selected organic pollutants from water. *International Journal of Chemical Sciences* 2014; **12(3)**, 815-844.

[45] EJ Sullivan, WJ Carey and RS Bowman. Thermodynamics of cationic surfactant sorption onto natural clinoptilolite. *Journal of Colloid and Interface Science* 1998; **206(2)**, 369-380.

[46] S Bhattacharjee. DLS and zeta potential - what they are and what they are not? *Journal of Controlled Release* 2016; **235**, 337-351.

[47] P Sennett and JP Oliver. Colloidal dispersion electrokinetic effects and the concept of zeta potential. Industrial & *Engineering Chemistry* 1965; **57(8)**, 32-50.

[48] A Al-Mamoori, M Alsalbokh, S Lawson, AA Rownaghi and F Rezaei. Development of bismuth-mordenite adsorbents for iodine capture from off-gas streams. *Chemical Engineering Journal* 2020; **391**, 123583.

[49] FS Wanyonyi, F Orata, GK Mutua, MO Odey, S Zamisa, SE Ogbodo, F Maingi and A Pembere. Application of south african heulandite (HEU) zeolite for the adsorption and removal of Pb2+ and Cd2+ ions from aqueous water solution:

experimental and computational study. *Heliyon* 2024; **10(14)**, e34657.

[50] FK Mostafapour, M Yilmaz, AH Mahvi, A Younesi, F Ganji and D Balarak. Adsorptive removal of tetracycline from aqueous solution by surfactant-modified zeolite: Equilibrium, kinetics and thermodynamics. *Desalination and Water Treatment* 2022; **247**, 216-228.

[51] N Patdhanagul, T Srithanratana, K Rangsriwatananon and S Hengrasmee. Ethylene adsorption on cationic surfactant modified zeolite NaY. *Microporous and Mesoporous Materials* 2010; **131(1-3)**, 97-102.

[52] P Hałas, D Kołodyńska, A Płaza, M Gęca and Z Hubicki. Modified fly ash and zeolites as an effective adsorbent for metal ions from aqueous solution. *Adsorption Science & Technology* 2017; **35(5-6)**, 519-533.

[53] M Dmvila-Estrada, JJ Ramirez-Garcia, MJ Solache-Rios and JL Gallegos-Perez. Kinetic and equilibrium sorption studies of ceftriaxone and paracetamol by surfactant-modified zeolite. *Water Air Soil & Pollution* 2018; **229(4)**, 123.

[54] N Ayawei, AN Ebelegi and D Wankasi. Modelling and interpretation of adsorption isotherms. *Journal of Chemistry* 2017; **2017(1)**, 3039817.

[55] H Li, Z Fu, L Yang, C Yan, L Chen, J Huang and Y Liu. Synthesis and adsorption property of hydrophilic–hydrophobic macroporous crosslinked poly(methyl acryloyl diethylenetriamine)/poly(divinylbenzene) (PMADETA/PDVB) interpenetrating polymer networks (IPNs). *RSC Advances* 2015; **5(34)**, 26616-26624.

[56] M Essandoh, B Kunwar, CU Pittman, D Mohan and T Mlsna. Sorptive removal of salicylic acid and ibuprofen from aqueous solutions using pine wood fast pyrolysis biochar. *Chemical Engineering Journal* 2015; **265**, 219-227.

[57] K Mphahlele, MS Onyango and SD Mhlanga. Adsorption of aspirin and paracetamol from aqueous solution using Fe/N-CNT/β-Cyclodextrin nanocomopsites synthesized via a benign microwave assisted method. *Journal of Environmental Chemical Engineering* 2015; **3(4)**, 2619-2630.

[58] S Wong, Y Lee, N Ngadi, IM Inuwa and NB Mohamed. Synthesis of activated carbon from spent tea leaves for aspirin removal. *Chinese Journal of Chemical Engineering* 2018; **26(5)**, 1003-1011.